




Improvement of Power Quality in Grid Integrated Smart Grid Using Fractional-Order Fuzzy Logic Controller

D Chandra Sekhar*, PVV Rama Rao**, R Kiranmayi***

*Department of EEE, JNTUA, Ananthapuramu, India

**Department of EEE, MVSR Engineering College, Hyderabad, India

*** Department of EEE, JNTUA, Ananthapuramu, India

(dcsekhar@mrec.ac.in, pvvmadhuram@gmail.com, kiranmayi0109@gmail.com)

†

D Chandra Sekhar; dcsekhar@mrec.ac.in

Received: 05.04.2022 Accepted: 07.05.2022

Abstract- This paper investigates a fractional-order Fuzzy logic controller (FOFLC) for improving the performance of the Smart Grid. The proposed FOFLC improves the steady-state and transient performance of the solar-wind-grid integrated system. Fuzzy maximum power point tracking (MPPT) algorithm-based DC-DC converters are used to get the most power out of solar panels. A permanent magnet synchronous generator (PMSG) is used to extract the most power from the wind. An intelligent FOFLC controller controls back-to-back voltage source converters (VSC) to optimize both power generation. This proposed methodology was implemented by optimal power converters, which improved the overall system performance to an acceptable level. The simulation results show that the proposed control method works well for a wide range of smart grid modes and non-linear fault scenarios. From the simulations it is clear that the current's harmonic content is reduced by 1.04% to 0.67% and voltage harmonics is reduced 8.31% to 0.31% in FOFLC in contrast to ANFIS controller.

Keywords FOFLC; Maximum power point tracking, Power quality, PV-wind-grid integration, MATLAB/Simulink,

1. Introduction

In recent years the usage of renewable energy sources (RES) is popular over traditional fossil fuel-based energy sources like hydro and thermal. RES sources are free from air pollutants (eco-friendly), with more reliability and optimum cost. To extract maximum power from solar different MPPT algorithms are proposed in the literature such as perturb and observe [1], incremental conductance (IC), and fuzzy intelligent Maximum power point tracking (MPPT) [2]. In this paper to get maximum power from photovoltaic (PV), the fuzzy MPPT technique is adopted. Maximum power extracted from the wind with tip-speed ratio control, lower relationship-based, perturbation and observation (P&O), hybrid control [3] and intelligent control strategies [4], [5] based techniques like neural, fuzzy, and adaptive-neuro fuzzy interfaced system (ANFIS). Stand-alone integrated hybrid power sources [6], [7] are modeled and controlled well to satisfy the load demand [8]–[10]. It is further extended to dynamic energy management between the RES sources is proposed with conventional control techniques.

After doing a literature review, it was discovered that ANFIS is a popular controller due to its simplicity. As previously stated, it is frequently employed in power system applications. The filter parameter is the most difficult aspect of the ANFIS design. In real-time practice, this filter

parameter is tuned based on the user's requirements. We know that the advanced control state feedback control strategy is more versatile, allowing for optimal design [11]–[14].

A blend of neural and fuzzy rationale procedures offers to take care of issues and challenges in the plan fuzzy has been executed by [30]. The new methodology in the design of the neural organization is known as a recurrent neural network (RNN) which is an improvement over the current controllers and is actualized in [15] The yield of a dynamic framework is a component of a past yield or previous information or both, thusly recognizable proof and control of dynamic framework are an inborn errand contrasted with a static framework [15]–[20]. The feed-forward neural fuzzy organizations have a significant downside so their application is restricted to static planning issues [21]– [26]. In this way, to recognize dynamic frameworks, repetitive neuro-fuzzy organizations ought to be utilized. A TSK-type intermittent fuzzy organization is intended for dynamic frameworks [27-30].

In light of the audit, it is presumed that the motions in the dynamic power frameworks can be damped by the versatile fuzzy controller. The exploration work is done to check the presentation of FACTS devices for upgrading framework execution. The FOFLC is proposed for the power stabilizer. The PID, as ANFIS controller boundaries are prepared by particle swarm optimization (PSO). The FOFLC can be made as a self-learning controller utilizing an iterative learning

strategy clarified. Developmental calculations are equal and worldwide pursuit methods. Since they all the while assessing numerous focuses in the inquiry space, they are bound to unite toward the worldwide arrangement clarified.

The next sections of this article are composed of the system configuration PV wind integrated grid in section 2. The proposed FOFL control scheme is in section 3. MATLAB environmental-based simulation results are shown in section 4 and the conclusion is given in section 5.

The main objective of the methodology is to implement optimal power converters, which improved the overall system performance to an acceptable level.

2. System Configuration

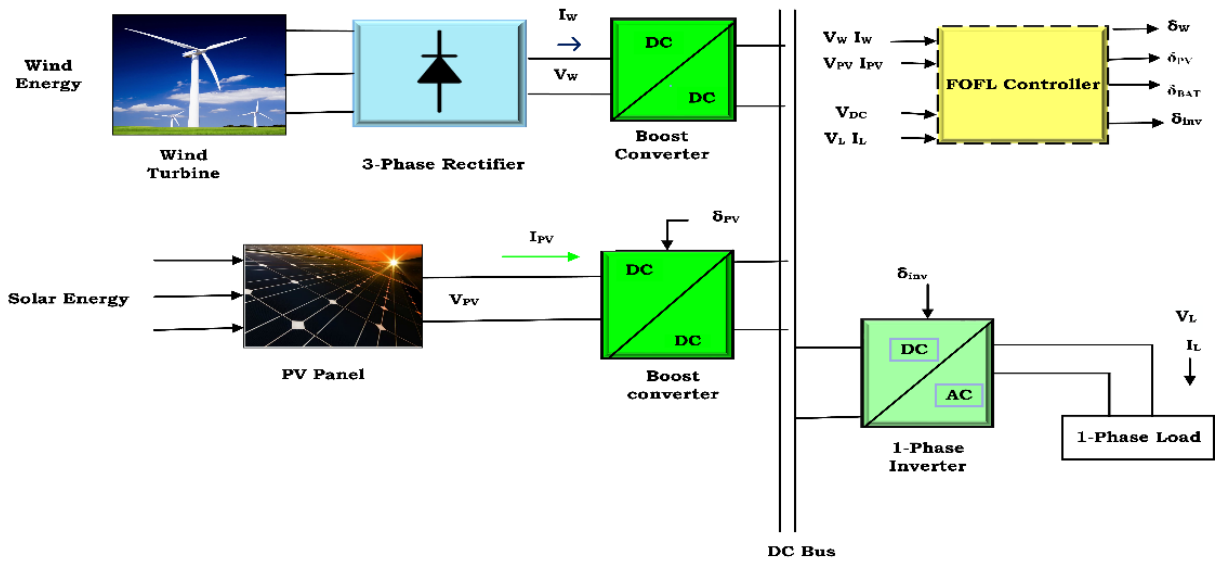


Fig. 1. Model of proposed PV-wind integrated grid

2.1. Design of Photo Voltaic Cell

The design of a solar cell in general is connected by a I_{LGC} in parallel with a diode and resistors which are associated in anti-parallel which is shown in Figure 2 and control solar cell power.

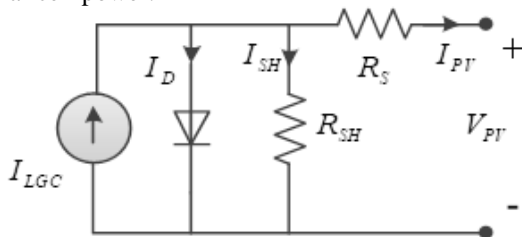


Fig.2. Representation diagram of PV cell

In the figure, PV panels are connected in an array to generate the desired output voltage and current, and the voltage, current are given mathematically;

$$V_{series} = \sum_{j=1}^n V_j = V_1 + V_2 + \dots + V_n \quad (1)$$

A model of a grid-integrated solar-wind smart grid system is shown in Figure 1. Smart grid systems must optimize performance, dependability, and operational efficiency. This study creates a novel model of a smart grid-connected PV/WT hybrid system. A photovoltaic array, wind turbine, asynchronous (induction) generator, controller, and converters are all part of the system. The model is created using the MATLAB/Simulink software suite. Based on the construction of an MPPT, the P&O technique is employed to maximize the generated power. The recommended model's dynamic behavior is investigated in a range of operational circumstances.

$$V_{seriesoc} = \sum_{j=1}^n V_j = V_{oc1} + V_{oc2} + \dots + V_{ocn} \text{ for } I = 0 \quad (2)$$

$$I_{parallel} = \sum_{j=1}^n I_j = I_1 + I_2 + \dots + I_n \quad (3)$$

$$V_{parallel} = V_1 = V_2 = \dots = V_n \quad (4)$$

By default, bypass diodes are used in solar panels to reduce overvoltage in the system. However, it raises the expense of the system.

2.2. DC-DC Converters

A fuzzy MPPT algorithm is now employed to regulate the switching pattern in order to attain the PV module's maximum power output. The dynamic performance and overall efficiency of the PS network are improved by this fuzzy logic controller (FLC) based direct current (DC) converter, which sends less oscillating voltage to the series VSCs[29].

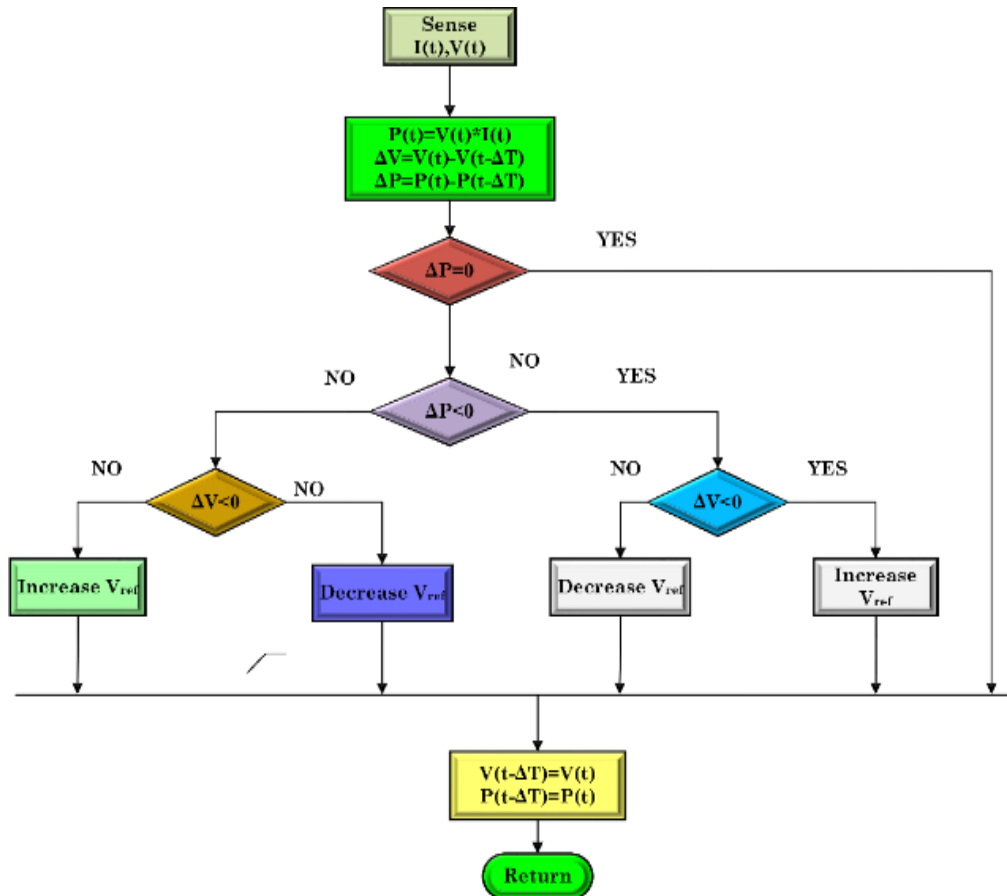


Fig.3. MPPT Algorithm

If $i_d=0$, the electromagnetic torque is described as in (8).

$$T_e = \frac{3}{2} P n \psi f i_q \tag{8}$$

The dynamic equation of wind turbine is described by (9).

$$J \frac{d\omega_m}{dt} = T_e - T_m - F \omega_m \tag{9}$$

3. Control Scheme

The FLC MPPT approach is comparable to the construction of FLC based voltage source inverters (VSI). This blunder is viewed as a set of ill-defined guidelines. Figure 3 shows how to choose rules, membership functions, and defuzzification. The PI control parameters are provided by these fuzzy sets. Table 1 and Figure 4 The set of fuzzy rules is shown in Figure 4(a) error, Figure 4(b) change in error, and Figure 4(c) output membership functions. Fuzzy logic reasoning differs from traditional frameworks such as NB, NS, Z, PB, and PS in both concept and substance. The actual voltage across the coupling's (V_{dact}) point differs from the reference V_{dc} , resulting in an error that is fuzzified, rectified, and transmitted to the scheme later de-fuzzification.

2.3. Design of Permanent Magnetic Synchronous Based Wind Energy

Because the permanent magnet synchronous generator (PMSG) is a brushless DC machine, it has a simple and durable design. When compared to the doubly-fed induction generator (DFIG) generator, it is less expensive. By adjusting terminal voltages of the PMSG's rotor circuit, it regulates the actual, reactive power of the wind energy conversion system (WECS) system. As a result, it regulates the power factor of the entire WECS. PMSG is used to accomplish desired speed management without the need for slip rings[28]. Mathematically PMSG represents in the dq0 axis:

$$V_{gq} = (R_g + p \cdot L_q) \cdot i_q + \omega_e \cdot L_d i_d \tag{5}$$

$$V_{gd} = (R_g + p L_d) \cdot i_d - \omega_e L_q i_q \tag{6}$$

where V_{gd} and V_{gq} represent the stator voltages in the direct and quadrature axis.

$$T_e = \frac{3}{2} P n [\phi + i_q - (L_d - L_q) i_d i_q] \tag{7}$$

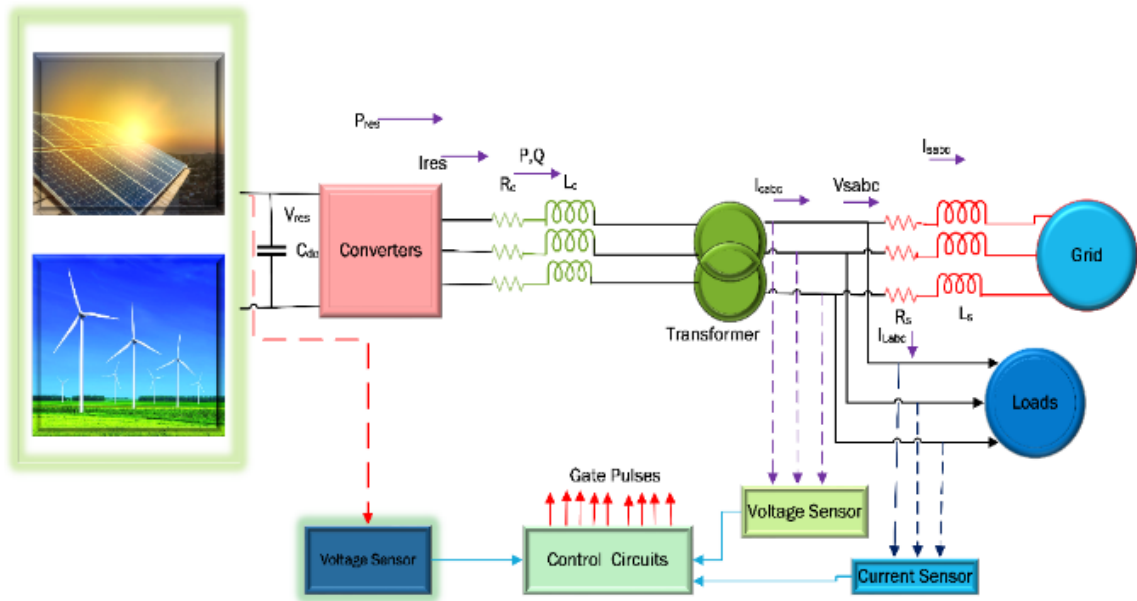


Fig. 4. Simulation diagram for the proposed model

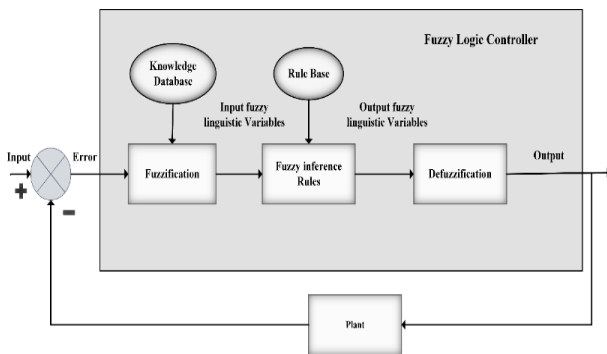


Fig. 5. Fuzzy inference system

Table 1. Rules set by Fuzzy Controller

		Error (E)						
		NB	NM	NS	Z	PS	PM	PB
Change in Error (ΔE)	NB	NB	NB	NB	NS	NS	NS	Z
	NS	NB	NM	NS	NS	Z	PS	PS
	Z	NS	NM	NS	Z	PS	PM	PM
	PS	NS	NS	Z	PS	PM	PB	PB
	PB	Z	NB	PS	PS	PB	PS	PB

3.1. VSI controller design by using FOFLC
 3.1.1. Fractional Order Fuzzy Logic Controller (FOFLC)

The FOFLC is very much famous to understand the derivative operator. The numerical expression for FOPI[24] is

$$C(s) = Kp + \frac{Ki}{s^\lambda} \tag{1}$$

λ is range of (0,1).

If $\lambda \geq 2$ is high-order value that is equal to the conventional controller. The F.O is mentioned in (1) is common character of PI controller. To resolve the issues in FOFL controller effective filters can be used. The fitting range is (ω_b, ω_h) . The fractional-order function [24] is

$$K(s) = (1 + bs/d\omega b)/(1 + bs/d\omega h) \tag{2}$$

Where $0 < \lambda < 1, s = j\omega, b > 0, d > 0$, and

$$K(s) = \left(\frac{bs}{d\omega b}\right)^\lambda \left(1 + \frac{-ds+d}{ds^2+b\omega h s}\right)^\lambda \tag{3}$$

In frequency range between $\omega b < \omega < \omega h$ by including Taylor polynomial expansion form which occurs

$$K(s) = (bs/d\omega b)^\lambda \left(1 + \lambda P(s) + \frac{\lambda(\lambda-1)}{2} p^2(s)\right) \tag{4}$$

$$\text{Here } p(s) = \frac{-ds^2+d}{ds^2+b\omega h s} \tag{5}$$

It is initiated that

$$S^\lambda = \frac{(d\omega b)^{\lambda b - \lambda}}{\left[1 + \lambda P(s) + \frac{\lambda(\lambda-1)}{2} p^2(s)\right]} \left(\frac{1 + \frac{bs}{d\omega b}}{1 + \frac{ds}{d\omega h}}\right)^\lambda \tag{6}$$

Estimated the Taylor polynomial leads to

$$S^\lambda = \frac{d\omega b}{b} \frac{ds^2+b\omega h s}{d(1-\lambda)s^2+b\omega h s+d\lambda} \left(\frac{1 + \frac{bs}{d\omega b}}{1 + \frac{ds}{d\omega h}}\right)^\lambda \tag{7}$$

The FO is defined as

$$S^\lambda = \frac{d\omega b}{b} \frac{ds^2+b\omega h s}{d(1-\lambda)s^2+b\omega h s+d\lambda} \left(\frac{1 + \frac{bs}{d\omega b}}{1 + \frac{ds}{d\omega h}}\right)^\lambda \tag{8}$$

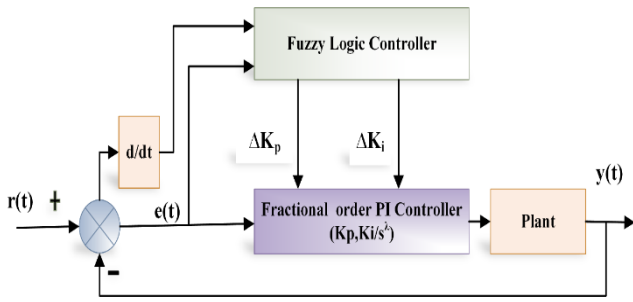
Equation (8) is balanced only when poles are located on left hand side of complex s-plane.

The poles of equation (8) are

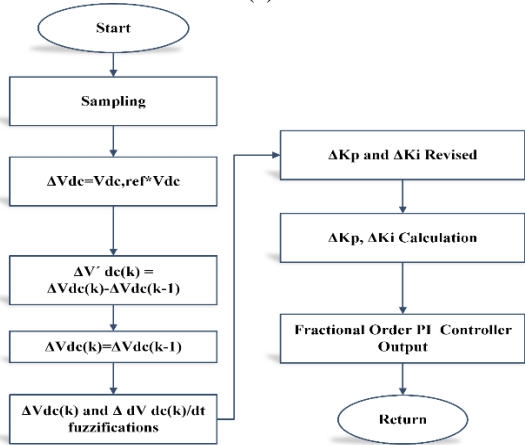
$$d(1-\lambda)s^2 + b\omega h s + d\lambda \tag{9}$$

The negative poles in real part for $0 < \lambda < 1$. The poles in equation (7) is in range of $(\omega | \omega h)$. The (6)th equation is approximated by uninterrupted -time coherent simulation [24].

$$K(s) = \lim_{n \rightarrow \infty} K_n(s) = \lim_{n \rightarrow \infty} = -N \frac{1 + \frac{s}{\omega k}}{1 + \frac{s}{\omega k}} \tag{10}$$

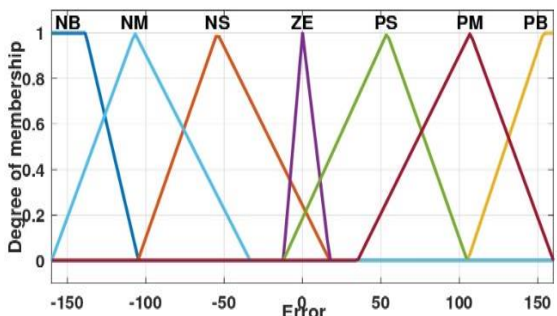


(a)

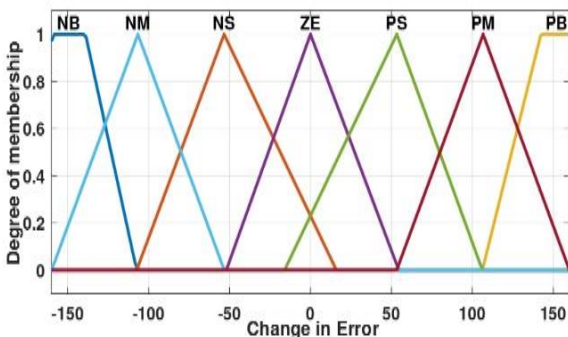


(b)

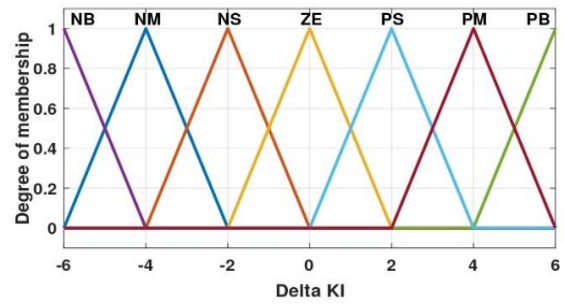
Fig. 6. (a) Control diagram of FOFL Controller (b) Flowchart



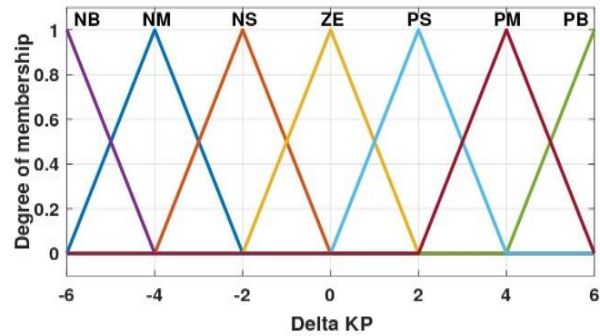
(a)



(b)



(c)



(d)

Fig.7. Membership function for (a) error, (b) change in error, and (c) ΔK_i (d) ΔK_p

The proposed fuzzy logic controller is shown in Figure 5. The proposed FLC has two input membership function, two output membership function which is shown in Figure 7. The gain values k_p, k_i are computed by using following equations

$$k_p = K_p + \Delta K_p \tag{11}$$

$$k_i = K_i + \Delta K_i \tag{12}$$

Here, k_p, k_i are initial values of gain FLC and $\Delta K_p, \Delta K_i$ are scaling factors from FLC. The proposed control structure is applicable for wind energy management systems where $V_{dc, ref}, I_{dc, ref}$ are inputs which are connected to K_p, K_i . The change in gain values can be derived from equations 11 & 12 respectively. Zero order band which is connected to FLC is used to approximate constants. The rule table for proposed control strategy is given in Table 1.

4. Simulation Results

The variation of DC link voltage (step response) is momentarily considered at point $t=1$ sec as shown in Figure 7. The variation of PV-wind power production based on its availability considered as shown in Figure 8. In PV cell irradiance considered as 1 kW/m^2 up to $t=0.3$, momentarily it is changed to 0.9 kW/m^2 , the time between 0.3 s to 0.5 s . At $t=0.5 \text{ s}$ to 0.6 s irradiance is 0.4 kW/m^2 decreases, and between $t=0.6 \text{ s}$ to $t=0.8 \text{ s}$ irradiance considered as 0.6 kW/m^2 . Similar variation of wind power generation is considered as 0.82 m/s to $t=2 \text{ ms}$. After wind is increased to 1.1 m/s in time between $t=2 \text{ s}$ to 4 sec . Further wind decreased

to 0.7 m/s time between $t=4$ s to $t=6$ s and wind increases to drastically up to 1.2 m/s from time between $t=6$ s to $t=8$ s.

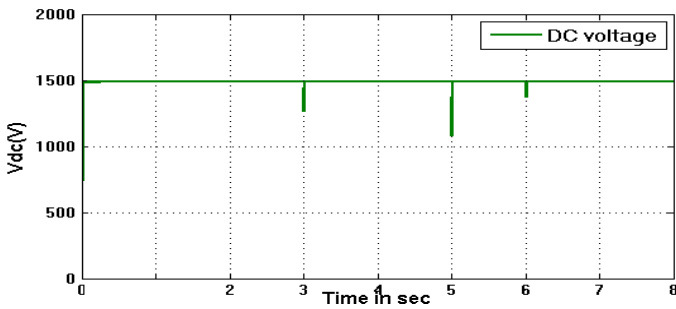


Figure.7 Step variation of DC link voltage

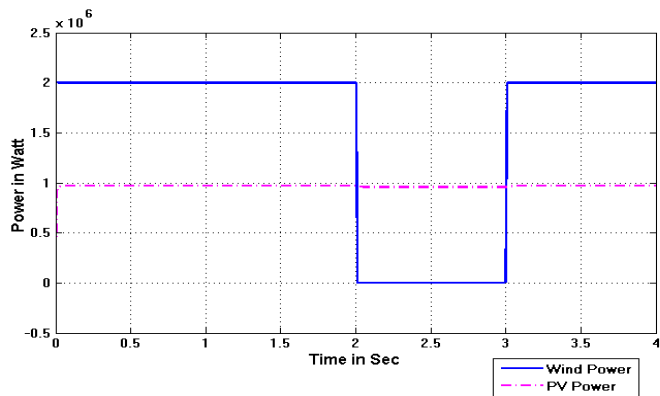
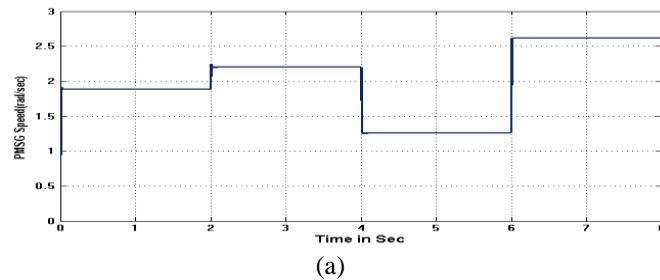


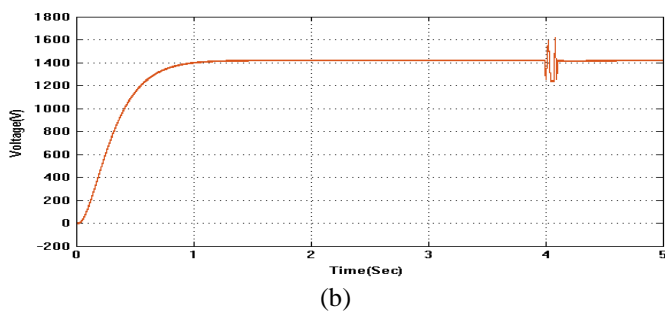
Fig. 8. Variation of solar-wind power generation

4.1. FOFLC Based VSI Controller Design

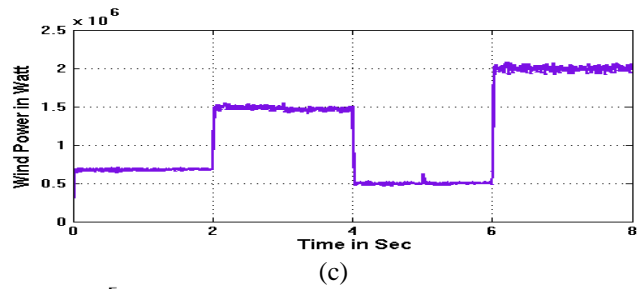
The performance of the smart grid with both PV-wind power generation is shown in Figures 9(a) to 9(g) those are PMSG speed, voltage at DC link capacitor, wind power, solar power, grid current, voltage across CPI, VSR modulation respectively. From the Figures 8(b) and 8(f) it is clear that fixed voltages are produced with even variable PV-wind power generation. Effective power management done between grid-PV-wind (smart grid) with employing ANFIS operated VSC converters.



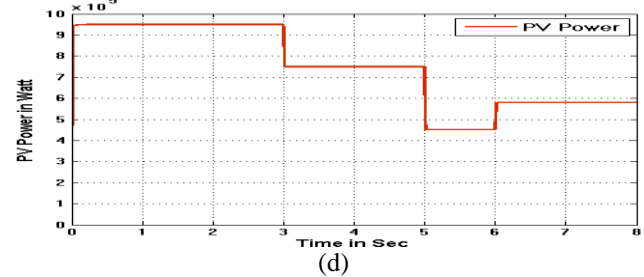
(a)



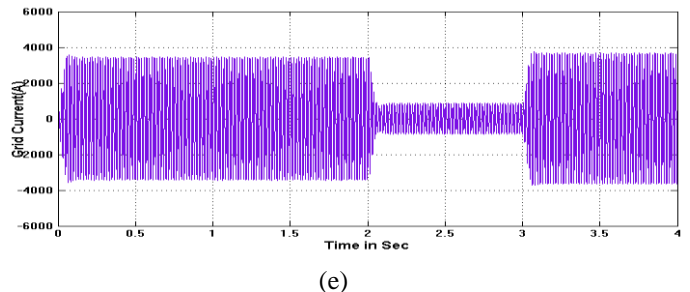
(b)



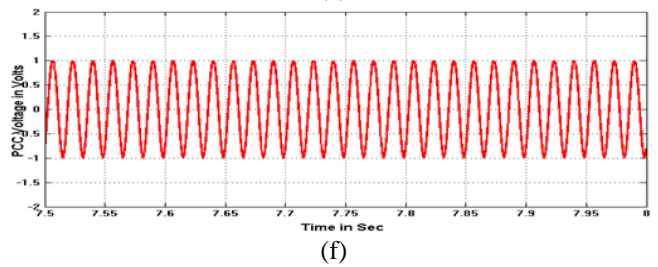
(c)



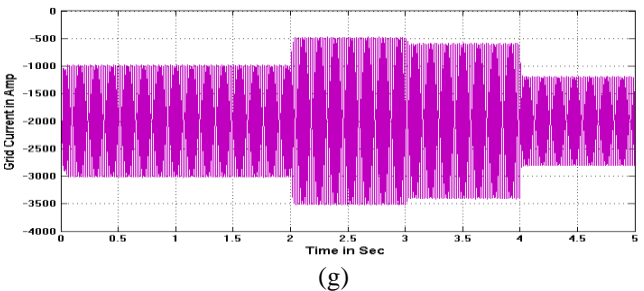
(d)



(e)



(f)



(g)

Fig. 9. Performance of the smart grid with both PV-wind power generation (a) PMSG speed (rad/sec), (b) DC link voltage, (c) wind power (W), (d) solar power (W), (e) grid current, (f) voltage at CPI, and (g) VSR modulation

4.2. Performance of the System Only with Wind Power Generation

The energy management of the smart-grid only with wind is described in this session. In this low or zero irradiance (during night) appearances power establishment done by solar is minimum. In this situation wind energy is only prime responsible to reach the load demand. The output simulation

results are illustrated in Figures 10(a) to 10(c). Those are wind speed, wind power and grid current respectively.

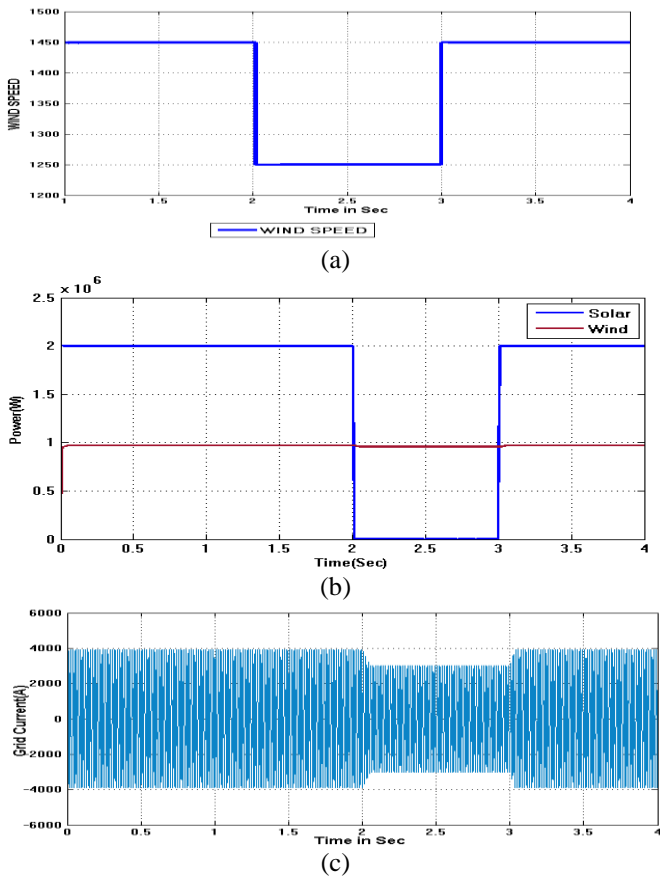
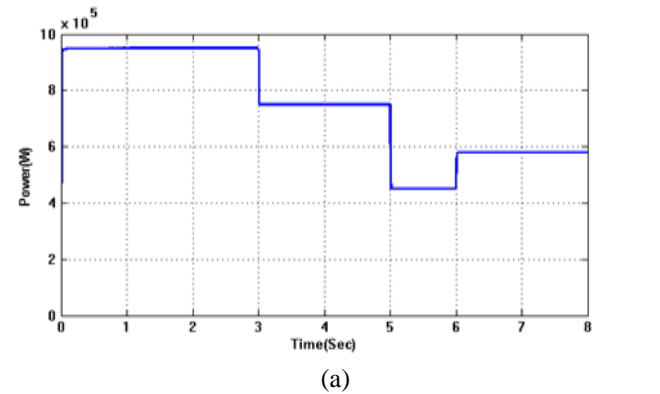


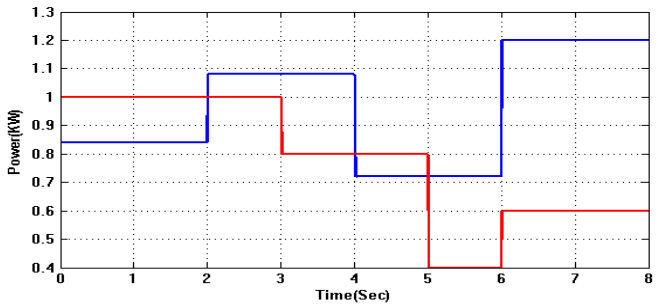
Fig.10. Simulation results of the system only with wind power generation (a) wind speed, (b) wind power, and (c) grid current

4.3. Performance of the System Only With Solar Power Generation

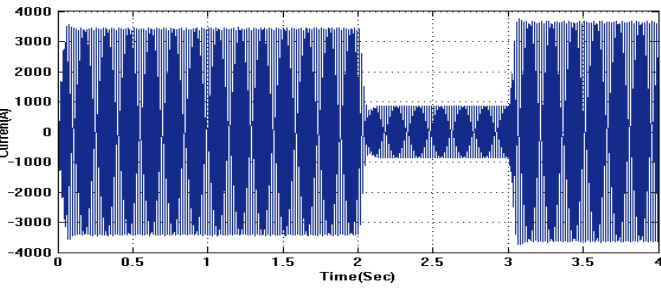
In this scenario, the smart grid's performance with solar electricity and low wind power generation is studied. Figure 11 depicts the output simulation results and their performance. Wind power, solar power, and grid current are depicted in Figures 11(a) to 11(c)



(a)



(b)



(c)

Fig. 11. Simulation result of (a) wind speed (b) solar power and (c) grid current

4.4. Performance of the system with symmetrical fault

From Figure 12 comparison of DC link voltage with protection controller and without controller it clear that with using proposed technique the oscillations occurred in grid current is less.

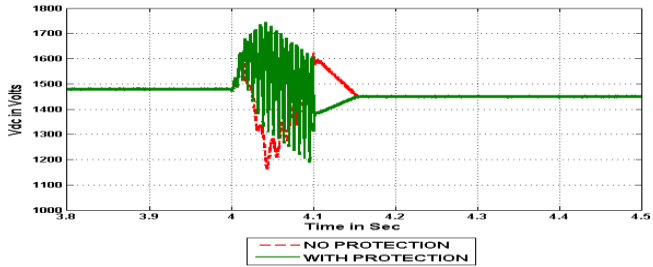


Fig. 12. DC link voltage with and without protection

It is mitigated within the first four cycles. Total harmonic distortion (THD) of grid current and grid voltage of conventional controller and proposed controller is shown in Figure 13. Comparison THD for grid current with Figure 13(a) ANFIS controller and Figure 13(b) proposed controller and shown in Figure 14. Comparison THD for grid voltage with Figure 14(a) ANFIS controller Figure 14(b) proposed controller respectively.

The results demonstrate that with the FOFL controller, grid current THD is percent and grid voltage THD is percent. This controller can also adjust for all parameters effectively. As a result, the FOFL controller is the most effective of the ANFIS controllers that have been designed. Table 2 shows a comparison of THD with ANFIS and FOFL controllers.

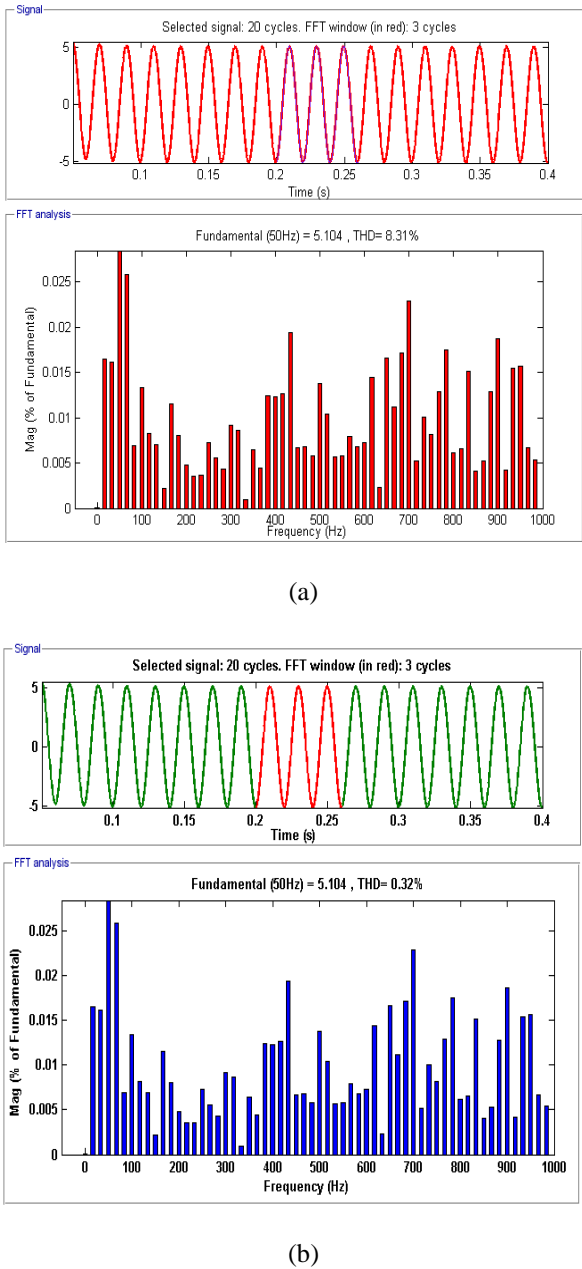


Fig. 13. THD for grid voltage comparison with (a) ANFIS controller and (b) proposed controller

Table 2. Comparison table for THD

S. No	Parameters	ANFIS Controller	Proposed Controller (FOFLC)
01	Grid Current	1.04%	0.67%
02	Grid Voltage	8.31%	0.31%

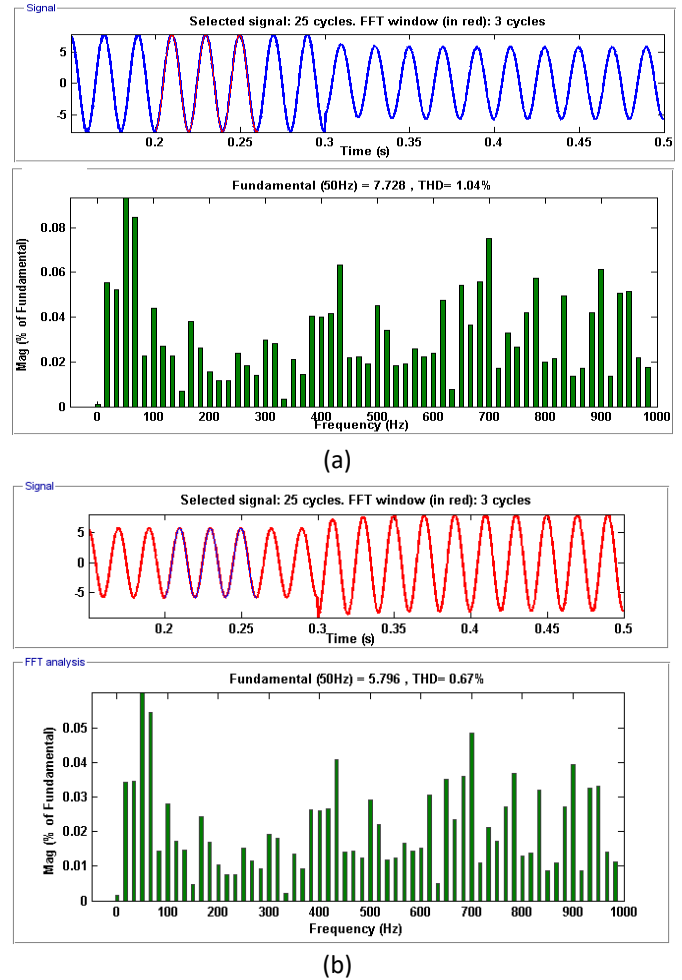


Fig. 14. THD for grid current comparison with (a) ANFIS controller and (b) proposed controller

5. Conclusion

This research investigates an efficient FOFL controller-based smart grid to improve power quality. Obtained simulation results for performance systems only with solar power and low wind energy, with wind energy and low solar power, and both solar-wind powers, are presented. From the simulations it is clear that the current's harmonic content is reduced by 1.04% to 0.67% and voltage harmonics are reduced from 8.31% to 0.31% in FOFLC in contrast to the ANFIS controller. In addition, it is observed that it has improved dynamic performance compared to the conventional control-based techniques like ANFIS controller, and individual loop control techniques. The proposed FOFL controller-based approach reduces network failure tolerance and improves the power quality. Future study could focus on how to improve the suggested method such that tracking errors are asymptotically stable, as well as how to improve control performance in the face of nonlinear inputs like load variations, and generation fluctuations and how to improve power quality in smart grids.

References

- [1] S. Salman, X. AI, and Z. WU, "Design of a P&O algorithm based MPPT charge controller for a stand-alone 200W PV system," *Protection and Control of Modern Power Systems*, vol. 3, no. 1, Dec. 2018, doi: 10.1186/s41601-018-0099-8.
- [2] D. Haji and N. Genc, "Fuzzy and P&O based MPPT controllers under different conditions," in 2018 7th International Conference on Renewable Energy Research and Applications (ICRERA), Oct. 2018, pp. 649–655, doi: 10.1109/ICRERA.2018.8566943.
- [3] B. Bhandari, S. R. Poudel, K.-T. Lee, and S.-H. Ahn, "Mathematical modeling of hybrid renewable energy system: A review on small hydro-solar-wind power generation," *International Journal of Precision Engineering and Manufacturing-Green Technology*, vol. 1, no. 2, pp. 157–173, Apr. 2014, doi: 10.1007/s40684-014-0021-4.
- [4] M. G. Simoes, B. K. Bose, and R. J. Spiegel, "Fuzzy logic based intelligent control of a variable speed cage machine wind generation system," in *Proceedings of PESC '95-Power Electronics Specialist Conference*, 1995, vol. 1, pp. 389–395, doi: 10.1109/PESC.1995.474840.
- [5] R. Chedid, F. Mrad, and M. Basma, "Intelligent control of a class of wind energy conversion systems," *IEEE Transactions on Energy Conversion*, vol. 14, no. 4, pp. 1597–1604, 1999, doi: 10.1109/60.815111.
- [6] T. Hirose and H. Matsuo, "Standalone hybrid wind-solar power generation system applying dump power control without dump load," *IEEE Transactions on Industrial Electronics*, vol. 59, no. 2, pp. 988–997, Feb. 2012, doi: 10.1109/TIE.2011.2159692.
- [7] K. Kant, C. Jain, and B. Singh, "A hybrid diesel-wind -PV-based energy generation system with brushless generators," *IEEE Transactions on Industrial Informatics*, vol. 13, no. 4, pp. 1714–1722, Aug. 2017, doi: 10.1109/TII.2017.2677462.
- [8] K. Sharma and D. K. Palwalia, "Robust controller design for DC-DC converters using fuzzy logic," in 2017 4th International Conference on Signal Processing, Computing and Control (ISPCC), Sep. 2017, pp. 477–481, doi: 10.1109/ISPCC.2017.8269726.
- [9] P. K. Ray, S. R. Das, and A. Mohanty, "Fuzzy-controller-designed-PV-based custom power device for power quality enhancement," *IEEE Transactions on Energy Conversion*, vol. 34, no. 1, pp. 405–414, Mar. 2019, doi: 10.1109/TEC.2018.2880593.
- [10] M. Bollen, J. Zhong, F. Zavoda, J. Meyer, A. McEachern, and F. Córcoles López, "Power quality aspects of smart grids," *Renewable Energy and Power Quality Journal*, vol. 1, no. 08, pp. 1061–1066, Apr. 2010, doi: 10.24084/repqj08.583.
- [11] S. Gheorghe, G. Gheorghe, N. Golovanov, and C. Stanescu, "Results of power quality monitoring in Romanian transmission and distribution system operators," in 2016 International Conference on Applied and Theoretical Electricity (ICATE), Oct. 2016, pp. 1–6, doi: 10.1109/ICATE.2016.7754628.
- [12] M. E. Ralph, "Control of the variable speed generator on the Sandia 34-m vertical axis wind turbine," presented at the Windpower '89 Conf. San Francisco, CA, 1989.
- [13] T. A. Lipo, "Variable speed generator technology options for wind turbine generators," NASA Workshop, Cleveland, 1984.
- [14] C. Nayar and J. H. Bundell, "Output power controller for a wind-driven induction generator," *IEEE Transactions on Aerospace and Electronic Systems*, vol. AES-23, no. 3, pp. 388–401, May 1987, doi: 10.1109/TAES.1987.310837.
- [15] P. G. Casielles, J. G. Aleixandre, J. Sanz, and J. Pascual, "Design, installation and performance analysis of a control system for a wind turbine driven self-excited induction generator," in *Proceedings ICEM '90*, 1990, pp. 988–993.
- [16] D. A. Torrey, "Variable-reluctance generators in wind-energy systems," in *Proceedings of IEEE Power Electronics Specialist Conference-PESC '93*, 1993, pp. 561–567, doi: 10.1109/PESC.1993.471982.
- [17] C. Brune, R. Spe, and A. K. Wallace, "Experimental evaluation of a variable-speed, doubly-fed wind-power generation system," in *Conference Record of the 1993 IEEE Industry Applications Conference Twenty-Eighth IAS Annual Meeting*, 1994, pp. 480–487, doi: 10.1109/IAS.1993.298967.
- [18] D. M. F. G. Roger, "IEEE recommended practice and requirements for harmonic control in electric power systems," *IEEE Std. 519-2014*, vol. 2014, 2014.
- [19] G. C. D. Sousa, B. K. Bose, and J. G. Cleland, "Fuzzy logic based on-line efficiency optimization control of an indirect vector-controlled induction motor drive," *IEEE Transactions on Industrial Electronics*, vol. 42, no. 2, pp. 192–198, Apr. 1995, doi: 10.1109/41.370386.
- [20] G. C. D. Sousa and B. K. Bose, "A fuzzy set theory based control of a phase-controlled converter DC machine drive," *IEEE Transactions on Industry Applications*, vol. 30, no. 1, pp. 34–44, 1994, doi: 10.1109/28.273619.
- [21] Krishna, D., M. Sasikala, and V. Ganesh. "Adaptive FLC-based UPQC in distribution power systems for power quality problems." *International Journal of Ambient Energy* 43, no. 1 (2022): 1719-1729.
- [22] P. E. Bett and H. E. Thornton, "The climatological relationships between wind and solar energy supply in Britain," *Renewable Energy*, vol. 87, pp. 96–110, Mar. 2016, doi: 10.1016/j.renene.2015.10.006.

- [23] D. Krishna, M. Sasikala, and V. Ganesh, "Mathematical modeling and simulation of UPQC in distributed power systems," in 2017 IEEE International Conference on Electrical, Instrumentation and Communication Engineering (ICEICE), Apr. 2017, pp. 1–5, doi: 10.1109/ICEICE.2017.8191886.
- [24] Krishna, D., Sasikala, M. & Kiranmayi, R. FOPI and FOFL Controller Based UPQC for Mitigation of Power Quality Problems in Distribution Power System. *J. Electr. Eng. Technol.* **17**, 1543–1554 (2022).
- [25] M. Saleh, Y. Esa, N. Onuorah and A. A. Mohamed, "Optimal microgrids placement in electric distribution systems using complex network framework," *2017 IEEE 6th International Conference on Renewable Energy Research and Applications (ICRERA)*, 2017, pp. 1036-1040, doi: 10.1109/ICRERA.2017.8191215.
- [26] Mhel, Hassan Raji, and Amina Mahmoud Shakir. "Total Harmonic Distortion Reduction of 9-Level Packed E-Cell (PEC9) Inverter." *International Journal of Smart Grid-ijSmartGrid* 6, no. 1 (2022): 13-22.
- [27] Sekhar, D. Chandra, PVV Rama Rao, and R. Kiranmayi. "Conceptual Review on Demand Side Management, Optimization Techniques for the Improvement of Power Quality in Smart Grids." In *2022 Second International Conference on Artificial Intelligence and Smart Energy (ICAIS)*, pp. 1640-1647. IEEE, 2022.
- [28] Mazouz, Farida, Sebti Belkacem, and Ilhami Colak. "DPC-SVM of DFIG Using Fuzzy Second Order Sliding Mode Approach." *International Journal of Smart Grid-ijSmartGrid* 5, no. 4 (2021): 174-182.
- [29] Y. Iwasaki, K. Yukita, T. Hosoe and K. Ikeda, "Basic study for the construction of a microgrid using small wind turbines as the main power source [PDF Not Yet Available In IEEE Xplore]," *2021 9th International Conference on Smart Grid (icSmartGrid)*, 2021, pp. 1-1, doi: 10.1109/icSmartGrid52357.2021.9551236.
- [30] A. A. Ameri, M. B. Camara and B. Dakyo, "Efficient Energy Management for Wind-Battery Hybrid System Based Variable Frequency Approach," *2021 10th International Conference on Renewable Energy Research and Application (ICRERA)*, 2021, pp. 125-130, doi: 10.1109/ICRERA52334.2021.9598696.